Evaluation of Performance Criteria for Simulation of Submaximal Steady-State Cycling Using a Forward Dynamic Model

R. R. Neptune
Human Performance Laboratory,
Faculty of Kinesiology,
University of Calgary,
Calgary, AB T2N 1N4

M. L. Hull
Department of Mechanical Engineering,
University of California, Davis,
Davis, CA 95616

The objectives of this study were twofold. The first was to develop a forward dynamic model of cycling and an optimization framework to simulate pedaling during submaximal steady-state cycling conditions. The second was to use the model and framework to identify the kinetic, kinematic, and muscle timing quantities that should be included in a performance criterion to reproduce natural pedaling mechanics best during these pedaling conditions. To make this identification, kinetic and kinematic data were collected from 6 subjects who pedaled at 90 rpm and 225 W. Intersegmental joint moments were computed using an inverse dynamics technique and the muscle excitation onset and offset were taken from electromyographic (EMG) data collected previously (Neptune et al., 1997). Average cycles and their standard deviations for the various quantities were used to describe normal pedaling mechanics. The model of the bicycle-rider system was driven by 15 muscle actuators per leg. The optimization framework determined both the timing and magnitude of the muscle excitations to simulate pedaling at 90 rpm and 225 W. Using the model and optimization framework, seven performance criteria were evaluated. The criterion that included all of the kinematic and kinetic quantities combined with the EMG timing was the most successful in replicating the experimental data. The close agreement between the simulation results and the experimentally collected kinetic, kinematic, and EMG data gives confidence in the model to investigate individual muscle coordination during submaximal steady-state pedaling conditions from a theoretical perspective, which to date has only been performed experimentally.

Introduction

Optimal control analysis of human movement has proven to be a powerful method to study multijoint movements with respect to muscle function and coordination. Optimal control analysis allows the researcher to study the dynamic musculoskeletal system by solving for the system control variables (e.g., muscle excitations) that satisfy the desired motor task and system constraints. This type of analysis provides a wealth of information such as individual muscle kinetics, kinematics, and coordination strategies. Optimal control analysis has been applied to the study of gait (e.g., Davy and Audu, 1987; Yamaguchi, 1990), jumping (e.g., Hatze, 1977; Pandy and Zajac, 1991) and other multijoint movements (e.g., Audu and Davy, 1985; Pandy et al., 1995).

Optimal control analysis has also been applied to forward dynamic simulation studies of cycling to examine, theoretically, equipment setup problems and muscle coordination of the lower extremity muscles (e.g., Kautz and Hull, 1995; Raasch et al., 1997). The constrained cyclical movement of pedaling allows for a controlled investigation of muscle coordination under a variety of test conditions (e.g., varied pedaling rate and workrate). Kautz and Hull (1995) developed a simulation of pedaling using net joint torque actuators to study endurance cycling. Although their study was successful in evaluating an equipment setup problem for improved performance, their study clearly indicated the need to model muscle mechanics and energetics explicitly by including individual muscle actuators in the system rather than net joint torques. Previous work in cycling using individual muscle actuators has focused on unambiguous performance criteria such as maximum-speed pedaling (Sim, 1988; Raasch et al., 1997) or maximum power output (Yoshihuku and Herzog, 1990; Bogert and Soest, 1993). But to date, no theoretical work in cycling using forward dynamic simulations with individual muscles has examined submaximal steady-state or "normal" endurance cycling conditions such as 90 rpm and 225 W (Hull et al., 1992). Therefore, the objectives of this study were: (1) to develop a forward dynamic model of cycling and an optimization framework to study pedaling under normal cycling conditions; and (2) to use the model and framework to identify the performance criterion that best reproduces normal pedaling mechanics for these conditions.

Methods

Bicycle-Rider Model. A planar two-legged bicycle-rider model was developed using SIMM (Fig. 1; MusculoGraphics, Inc., Evanston, IL). Each leg consisted of three rigid-body segments (thigh, shank, and foot) with the hip joint center fixed and foot rigidly attached to the pedal. All joint rotations were modeled as revolute except the knee, which had two translational degrees of freedom specified as functions of knee flexion angle (Yamaguchi and Zajac, 1989). Constrained to follow a path specified by the knee flexion angle (Delp et al., 1990), the patella served as the insertion point for the quadriceps muscles. The model was driven by 15 individual musculotendon

Contributed by the Bioengineering Division for publication in the JOURNAL OF BIOMECHANICAL ENGINEERING. Manuscript received by the Bioengineering Division September 20, 1996; revised version received October 23, 1997. Associate Technical Editor: A. G. Erdman.

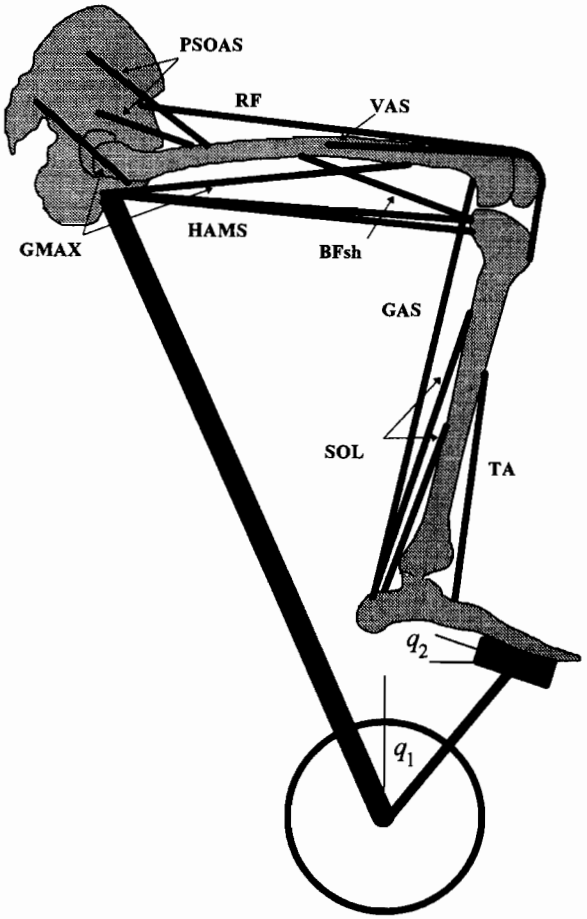

Fig. 1 Right leg of the bicycle-rider model. Muscles are shown as straight lines for illustration purposes. The 15 muscles used in the model were further combined into muscle sets, with each muscle within each set receiving the same excitation signal. The muscle sets were defined as PSOAS (iliacus, psoas), GMAX (gluteus maximus, adductor magnus), VAS (three-component vastus), HAMS (medial hamstrings, biceps femoris long), SOL (soleus, other plantarflexors), BFsh (biceps femoris short), GAS (gastrocnemius), RF (rectus femoris) and TA (tibialis anterior).

actuators per leg. The musculoskeletal geometry was based on the work of Delp et al. (1990). The crankload dynamics were modeled by an equivalent inertial and resistive torque applied about the center of the crankarm (Fregly, 1993).

The force-generating capacity of each muscle was based on a Hill-type model governed by the muscles' force-length-velocity characteristics (Zajac, 1989). Passive damping was added to the force-velocity relationship to make it invertible (Schutte et al., 1993). The musculotendon force applied to the corresponding segments was computed from the tendon strain by first computing muscle fiber length (Schutte et al., 1993). Therefore, the state equation for the muscle actuators was:

$$\dot{\mathbf{l}}^m = f(\mathbf{l}^m, \mathbf{q}, \dot{\mathbf{q}}) \tag{1}$$

where $\mathbf{l}^m$ is the vector of muscle lengths and $\mathbf{q}$ is the vector of the three generalized coordinates (defined as the crank and two pedal angles). The normalized muscle force-length, force-velocity, tendon stress-strain relationships, and maximum muscle contraction velocity were assumed constant for all muscles. The 15 muscles per leg included in the model were a subset of the muscles available in SIMM, which contribute to sagittal plane motion. Muscles with PCSA values greater than 14 cm^2 were selected and then lumped into "equivalent" muscles and further combined into muscle sets, with muscles within each set receiving the same excitation level (Raasch et al., 1997). The peak isometric force in each "equivalent" muscle was adjusted so that the torque-angle curve matched the summed torque-angle curves of the lumped muscles. Individual muscle model parameters are listed in Table 1 (Delp et al., 1990; Raasch et al., 1997).

The musculotendon kinematics were computed based on the lines of action of the 15 muscles (Delp et al., 1990). Joint angle dependent intermediate points were introduced when the origin and insertion points were not sufficient to describe anatomically correct muscle paths. These intermediate points were necessary in situations where the muscle either wraps over a bony prominence or is constrained by adjacent muscles.

Each of the 15 muscle actuators was stimulated by muscle activation coupled to the neural excitation ($\mathbf{a}^m$) through a first-order differential equation (Raasch et al., 1997), with activation and deactivation time constants of 50 and 65 ms, respectively (Winters and Stark, 1988), as:

$$\dot{\mathbf{a}}^m = \begin{cases} (\mathbf{u}^m - \mathbf{a}^m)\cdot(c_1\mathbf{u}^m + [c_2 \ldots c_2]^T) & \mathbf{u}^m \geq \mathbf{a}^m \\ (\mathbf{u}^m - \mathbf{a}^m)\cdot c_2 & \mathbf{u}^m < \mathbf{a}^m \end{cases} \tag{2}$$

where c_1 and c_2 are functions of the activation and deactivation time constants with $c_1 = \tau_{act}^{-1} - \tau_{deact}^{-1}$ and $c_2 = \tau_{deact}^{-1}$. The neural excitations ($\mathbf{u}^m$) were modeled as block patterns defined by duration and magnitude.

The dynamic equations of motion for the bicycle–rider system were derived using SD/FAST (Symbolic Dynamics, Inc., Mountain View, CA) and a forward dynamic simulation was produced by Dynamics Pipeline (MusculoGraphics, Inc., Evanston, IL). The equations of motion are presented in matrix form as:

$$\mathbf{M}(q)\ddot{q} = \mathbf{V}(q, \dot{q}) + \mathbf{G}(q) + \mathbf{D}^m\cdot\mathbf{F}^m(q, \dot{q}, a^m, l^m) + \mathbf{T}(q, \dot{q}) \tag{3}$$

where

q = generalized coordinates
$\mathbf{M}(q)$ = system mass matrix
$\mathbf{V}(q, \dot{q})$ = Coriolis and centripetal effects
$\mathbf{G}(q)$ = gravitational terms
$\mathbf{D}^m$ = muscle moment arm matrix
$\mathbf{F}^m(q, \dot{q}, a^m, l^m)$ = musculotendon actuator forces
a^m = muscle activations
l^m = muscle lengths
$\mathbf{T}(q, \dot{q})$ = friction terms

These equations represent three second-order differential equations corresponding to each of the degrees of freedom.

The performance criterion was composed to solve the "tracking" problem by minimizing the differences between experimental and model trajectory data. Specifically, the perfor-

Table 1 Musculotendon actuator parameters per leg

Muscle	Peak Isometric Force (N)	Optimal Fiber Length (m)	Tendon Slack Length (m)	Pennation Angle (deg)
BF-short	502	0.173	0.100	23
GAS	2225	0.045	0.408	17
GMAX				
Adductor Magnus	1250	0.131	0.260	5
Gluteus Maximus	1250	0.144	0.145	5
HAMS				
Medial Hamstrings	1698	0.080	0.359	15
Biceps Femoris Long	896	0.109	0.341	0
PSOAS				
Iliacus	788	0.100	0.090	7
Psoas	625	0.104	0.130	8
RF	974	0.084	0.346	5
SOL				
Soleus	3549	0.030	0.268	25
Other Plantarflexors	3250	0.031	0.310	12
TA	1375	0.098	0.223	5
VAS				
VAS-1	2125	0.087	0.221	3
VAS-2	2125	0.087	0.157	3
VAS-3	2125	0.087	0.081	3

mance criterion was the sum of squared residuals normalized by the intersubject variability in the general form of:

$$J = \sum_{j=1}^{m} \sum_{i=1}^{n} \frac{(Y_{ij} - \hat{Y}_{ij})^2}{SD_{ij}^2} \quad (4)$$

where

Y_{ij} = the experimentally measured data
$\hat{Y}_{ij}$ = the model data
n = number of time steps
m = number of tracking quantities evaluated
SD_{ij} = inter-subject standard deviation

In this criterion, variables with the least intersubject variability (i.e., more reproducible) were weighted more than the variables with greater variability. Specific tracking quantities included the crank and pedal kinetics and kinematics, intersegmental joint moments, and muscle excitation onset and offset timing.

The total system state equation in vector form was defined as:

$$[\dot{\mathbf{x}}]^T = [\dot{\mathbf{q}} \quad \dot{\mathbf{I}}^m \quad \dot{\mathbf{a}}^m]^T \quad (5)$$

with bounds on the control variables $\mathbf{u}$ (muscle excitations) such that:

$$0 \leq \mathbf{u}^m \leq 1 \quad (6)$$

A final time constraint was formulated to require an average pedaling rate of 90 ± 2 rpm.

Simulations were performed over four revolutions to assure that initial start-up transients had decayed. The final time constraints were not enforced until the fourth revolution when the simulation had reached its steady state and was considered to be independent of the initial conditions. Therefore, the simulation was not dependent on knowing the initial conditions a priori. Finally, the control strategies ($\mathbf{u}$) for the right and left leg were considered symmetric and 180 deg out-of-phase.

Thus, the optimal control problem was formulated to find the control vector $\mathbf{u}$ that minimizes the performance criterion (Eq. (4)) subject to the system state vector (Eq. (5)) and control bounds (Eq. (6)) while satisfying the final time constraint. The optimal control problem was solved by converting the optimal control formulation into a parameter optimization problem (Pandy et al., 1992). The controls (muscle excitation onset, offset, and magnitude) were optimized using a simulated annealing algorithm (Goffe et al., 1994), which minimized the tracking performance criterion while satisfying the final time constraint and control bounds. A schematic diagram of the optimization framework is presented in Fig. 2.

The seven performance criteria examined were:

$$J_1 = \sum_{i=1}^{n} \frac{(F_{xi} - \hat{F}_{xi})}{SD_{F_{xi}}^2} + \sum_{i=1}^{n} \frac{(F_{zi} - \hat{F}_{zi})^2}{SD_{F_{zi}}^2} \quad (7)$$

$$J_2 = \sum_{i=1}^{n} \frac{(T_{cranki} - \hat{T}_{cranki})^2}{SD_{T_{cranki}}^2} \quad (8)$$

$$J_3 = \sum_{i=1}^{n} \frac{(M_{ai} - \hat{M}_{ai})^2}{SD_{M_{ai}}^2} + \sum_{i=1}^{n} \frac{(M_{ki} - \hat{M}_{ki})^2}{SD_{M_{ki}}^2} + \sum_{i=1}^{n} \frac{(M_{hi} - \hat{M}_{hi})^2}{SD_{M_{hi}}^2} \quad (9)$$

$$J_4 = \sum_{i=1}^{n} \frac{(T_{cranki} - \hat{T}_{cranki})^2}{SD_{T_{cranki}}^2} + \sum_{i=1}^{n} \frac{(q_{2i} - \hat{q}_{2i})^2}{SD_{q_{2i}}^2} \quad (10)$$

$$J_5 = J_2 + J_3 \quad (11)$$

$$J_6 = J_1 + J_3 + J_4 \quad (12)$$

$$J_7 = J_6 + W \cdot \sum_{i=1}^{nmus} \sum_{j=1}^{2} \frac{(E_{ij} - \hat{E}_{ij})^2}{SD_{ij}^2} \quad (13)$$

where

q_2 = right pedal angle
F_x, F_z = right horizontal and vertical pedal force, respectively
T_{cranki} = crank torque
M_a, M_k, M_h = right ankle, knee, and hip intersegmental moments, respectively
E_{ij} = onset and offset timing of muscle i
W = weighting factor
$nmus$ = number of muscle sets

Criterion J7 was formulated to produce a simulation that tracked not only kinematic and kinetic quantities but also the muscle timing from experimental EMG data. W was chosen to weight the number of EMG data points (onset and offset timing for each muscle) equal to the number of data points in the other tracking quantities ($W = n/2nmus$).

Experimental Data. To provide data for the tracking problem, both kinetic and kinematic data were collected from six male competitive cyclists (avg and std dev of height = 1.79 ± 0.07 m; weight = 68.8 ± 7.6 kg; age = 22.2 ± 2.7 yr). Informed consent was obtained before the experiment. The subjects rode a conventional road racing bicycle adjusted to match their own bicycle's geometry. The bicycle was mounted on an electronically braked Schwinn Velodyne ergometer, which provided a constant workrate independent of pedaling rate. The protocol consisted of a 10 minute warm-up period at a workrate of 120 W at 90 rpm. Then, each subject cycled at a pedaling rate of 90 rpm and a workrate of 225 W. After a 2 minute adaptation period, data collection was randomly initiated during the following 2 minutes for 10 seconds.

The intersegmental moments were computed using a standard inverse dynamics approach (e.g., Hull and Jorge, 1985). The rider was modeled as a five-bar linkage in plane motion. The equations of motion for each link were solved using inverse dynamics, starting with the foot and proceeding through each link to the hip. The anthropometric estimates of each segment's mass and center of gravity were defined based on Dempster (1955). Moments of inertia were computed by the data presented in Wittsett (1963), which were personalized to each subject based on Dapena (1978).

The necessary kinematic data were recorded using a combination of video-based motion analysis and direct measurement. The intersegmental joint centers were obtained using a high-speed video system (Motion Analysis Corp., Santa Rosa, CA) from retroreflective markers located over the right anterior-superior iliac spine (ASIS), greater trochanter, lateral epicondyle, lateral malleolus, pedal spindle, and crank spindle. The hip joint center was located relative to the marker over the ASIS based on the methodology presented in Neptune and Hull (1995). The video data were filtered using a fourth-order zero phase shift Butterworth low pass filter with a cutoff frequency of 9 Hz. All derivatives to determine coordinate velocity and acceleration were calculated by fitting a quintic spline to the position data and differentiating the resulting equations.

The angular orientation data of the crank arm and pedal were measured with optical encoders and the pedal force data were measured with a pedal dynamometer described by Newmiller et al. (1988). The encoder and pedal force data were collected simultaneously with the video data at 100 Hz. Weight was added to the opposite pedal so that the inertial characteristics were similar. The pedal force and encoder data were filtered using a fourth-order zero phase shift Butterworth low pass filter with a cutoff frequency of 20 Hz. The filtered data were linearly interpolated to correspond in time with the video coordinate data. All tracking quantities were computed on a cycle-by-cycle

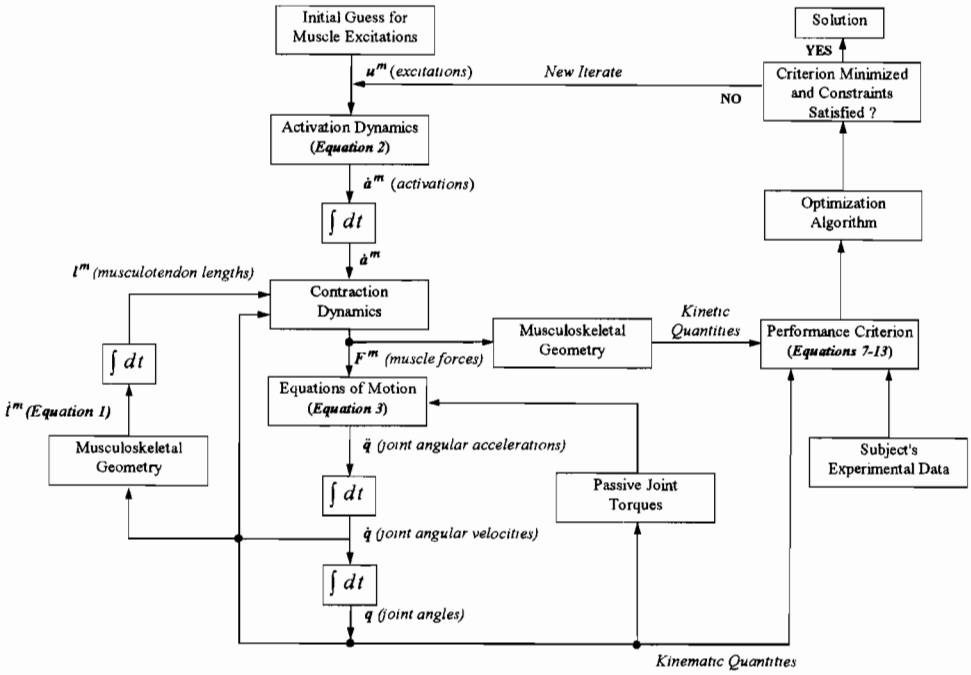

Fig. 2 Schematic diagram of the optimization framework. Note that the state vector elements are all simultaneously numerically integrated.

basis, averaged across cycles for each subject and then averaged across subjects.

Electromyographic (EMG) data collected in Neptune et al. (1997) under similar pedaling conditions provided the muscle timing defined by excitation onset and offset. The reader is referred to that manuscript for details on the data collection and processing. The EMG timing data for the hamstring muscle group (HAMS) were used to compute the EMG timing error for both the biceps femoris short head muscle (BFsh) and HAMS. No experimental EMG data were available for the PSOAS muscle so it was not included in the EMG error calculation.

Results

The pedaling simulation produced by tracking all the kinetic and kinematic quantities (J6) yielded the lowest total rms errors for these quantities and reproduced the subjects' data usually within ± 1 SD in all measured or computed kinetic and kinematic quantities [Figs. $3(a-g)$]. The horizontal and vertical pedal force, pedal angle, and crank torque profiles were almost always within ± 1 SD of the subjects' data [figs. $3(a-c)$]. The intersegmental joint moments were similar in both phasing and magnitude to the subjects' data except for the hip moment, which had a decrease in extensor moment near 180 deg [Figs. $3(e-g)$].

The simulation muscle excitation onset/offset timing produced by criterion J6 was similar with the onset/offset timing obtained from experimental EMG measurements (Neptune et al., 1997) [Fig. $4(a)$]. The power producing extensor muscles VAS, GMAX, and RF had close agreement except for the VAS onset and RF offset, which were later and earlier than the subjects, respectively. HAMS simulation timing was shifted later in the crank cycle while both GAS and TA compared well with the subjects. The short excitation burst by SOL during the late downstroke (140 deg to 165 deg) produced the largest timing difference of all muscles. The magnitude of the simulation muscle excitation compared well with the subjects' peak EMG data; all muscles were within 2 SD of the subjects, except GMAX and RF, which had over twice the magnitude [Fig. $5(a)$].

When the muscle timing was added to the tracking criterion together with all of the other kinetic and kinematic quantities (J7), the rms errors for the muscle timing decreased with only a small increase in the error for the kinetic and kinematic quantities. The net result was a slight decrease in the total rms error [Table 2]. The decrease in the error for the muscle timing was attributed largely to SOL whose onset was shifted earlier in the crank cycle to better match the subjects' experimental EMG data [Fig. $4(b)$]. The increase in the error for the kinetic and kinematic quantities was attributed primarily to the pedal angle, which deviated more from the subjects' data particularly during the first half of the upstroke region (180–270 deg) [Fig. $3(c)$]. However, the decrease in hip extensor moment near 180 deg noted for criterion J6 was now absent using criterion J7 [Fig. $3(g)$].

The only other performance criterion that compared well with criteria J6 and J7 by producing similar rms errors was criterion J4 which tracked the computed crank torque and measured pedal angle [Fig. 3, Table 2]. No other tracking criteria were as effective as criteria J4, J6, or J7 in minimizing the rms errors [Table 2], with total rms errors exceeding those of J6 by 20 to 60 percent.

Discussion

The primary objective of this study was to evaluate performance criteria within a dynamic optimization framework to identify the kinetic, kinematic, and muscle timing quantities necessary to best reproduce normal pedaling mechanics for steady-state cycling at 90 rpm and 225 W. To achieve this objective, a secondary objective was to develop a forward dynamic model of cycling and compare the simulation results to experimentally collected data from a representative sample of competitive cyclists during the same pedaling conditions.

To assess the robustness of the model, the sensitivity of the simulations to changes in model parameters was evaluated. The simulations were insensitive to the initial state (e.g., muscle length and velocity) since the tracking error was computed after the third cycle when the simulation had reached its steady state. Further, the simulations were insensitive to changes (± 10 percent) in the maximum isometric force. The model can compensate for inaccurate values of the maximum isometric force through the model's contraction dynamics by either increasing

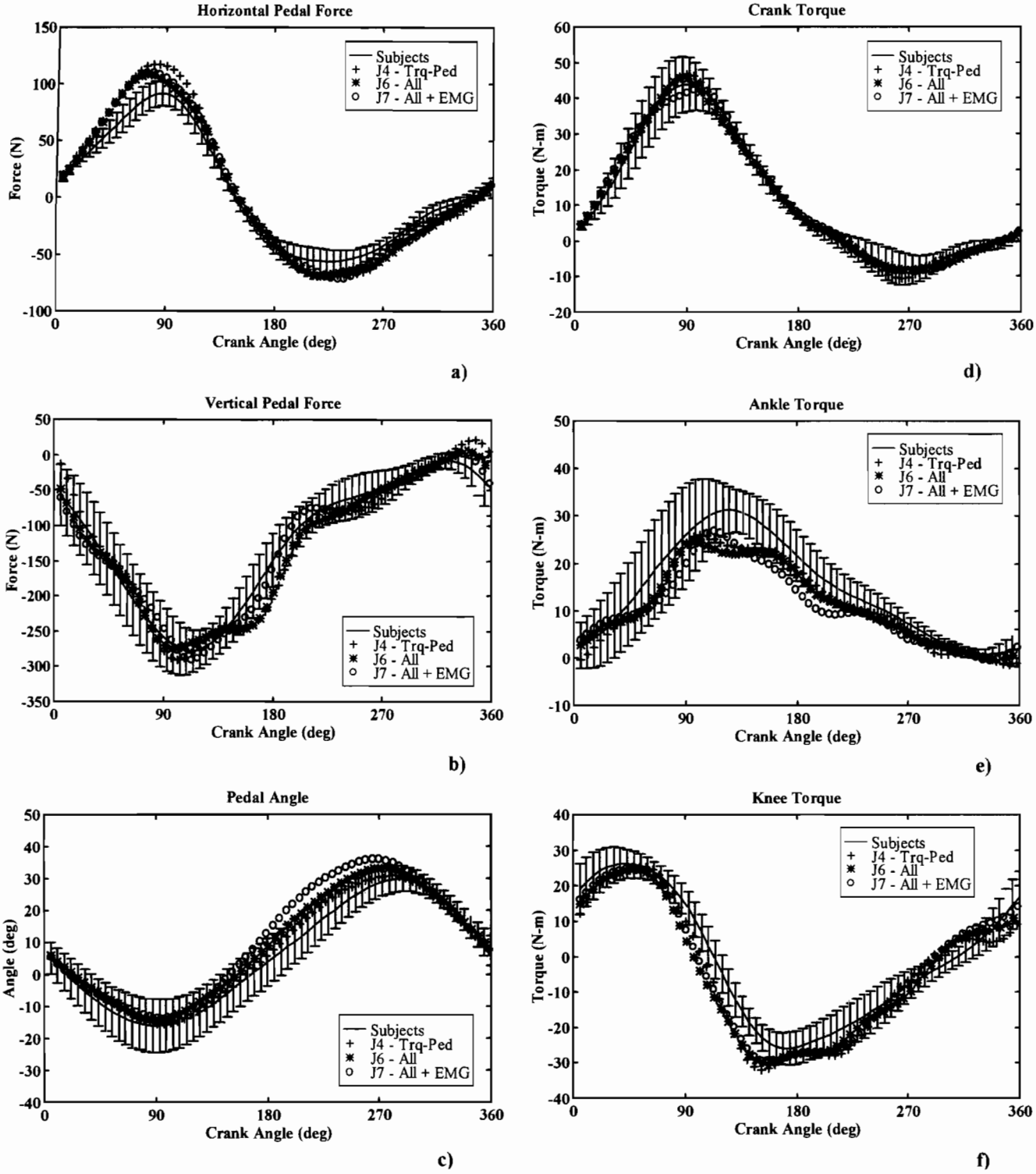

Fig. 3 Kinetic and kinematic quantities: (*a*) horizontal pedal force, (*b*) vertical pedal force, (*c*) pedal angle, (*d*) crank torque, (*e*) intersegmental ankle torque, (*f*) intersegmental knee torque, and (*g*) intersegmental hip torque. The crank angle is 0 deg at top-dead-center and positive in the clockwise direction. For the pedal force components, the horizontal force was defined as positive toward the front of the bicycle and the vertical component was positive upward. For the intersegmental moments, positive is extension and negative is flexion.

or decreasing the corresponding activation levels. Other SIMM specific model insensitivities have been identified elsewhere including subject height (Schutte et al., 1993) and activation and deactivation time constants (Piazza and Delp, 1996; Raasch et al., 1997).

The sensitivity of the muscle onset/offset timing was evaluated by performing an optimization with criterion J6 using the mean EMG onset/offset data from Neptune et al. (1997) initially and allowing the algorithm to vary the timing within ± 2 SD of the mean values. The results showed that the rms errors increased, but simulation results still reproduced the major features of pedaling. Similar model performance insensitivity to muscle timing was also reported in the maximum-speed pedaling study by Raasch et al. (1997).

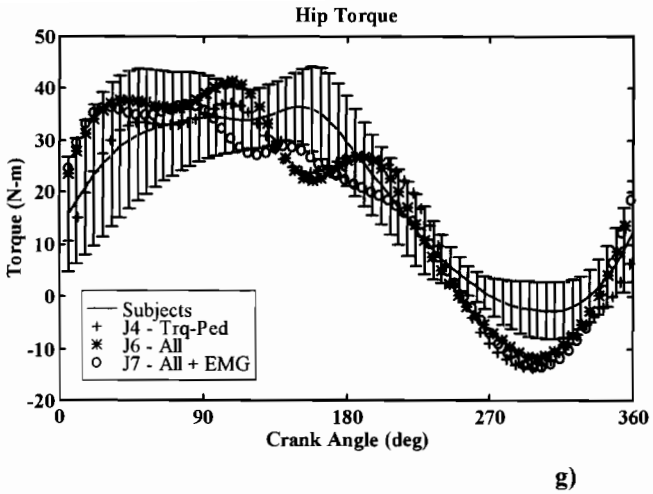

g)

Fig. 3 (Continued)

Fundamental to the success in solving the optimal control problem was the algorithm used within the optimization framework. The simulated annealing algorithm has been shown to improve convergence vastly over traditional gradient-based methods (Neptune and Bogert, 1997) and was insensitive to the initial values of the controls. The algorithm performs a random global search and avoids local optima by probabilistically accepting nonlocally optimum steps within the solution space. The algorithm converges on the most promising region as the "temperature" or step size decreases (Goffe et al., 1994). Thus, the initial controls had no influence on the resulting rms errors.

An assumption concerning the kinematics of the hip joint in the model and its possible influence on the tracking results also merits discussion. The model assumed that the hip joint was fixed while the kinematic data collected from the subjects contained hip motion. However, during the steady-state submaximal conditions of the present study (90 rpm, 225 W), the amount of hip motion was shown in a previous study to be minimal across a wide range of pedaling rates and workrates (Neptune and Hull, 1995). The difference in computed minimum, maximum, and average hip torque using the fixed hip assumption verses allowing hip motion was shown in that study to be less than 0.3 percent. Therefore, the fixed hip assumption was deemed to have no influence on the tracking results.

Having established the robustness of the model and optimization framework, the results showed that criterion J6 was able to reproduce the subjects' data usually within ± 1 SD in all of the measured or computed kinetic and kinematic quantities [Figs. 3(*a*–*g*)]. Despite the success of the model in reproducing the fundamental pedaling mechanics, differences between the simulation excitation timing and the experimental EMG data were apparent. The most profound difference was found in the timing of SOL [Fig. 4(*a*)]. The simulation excitation of SOL occurred in the late downstroke for a short duration (143–163 deg) while the subjects excited SOL early in the downstroke (350–132 deg). Substantial improvements were made in the SOL timing when experimental EMG timing was added to the tracking criterion [Fig. 4(*b*)]. Adding the EMG timing to the criterion reduced the muscle control redundancy (i.e., simultaneous excitation of different muscles) and substantially increased the period of SOL excitation, resulting in an improved match with the subjects' EMG data.

Criterion J7 not only improved the SOL timing, but also improved the timing match for GMAX, RF, HAMS, and TA excitations. Since tracking the external pedaling quantities (J6) does not explicitly consider muscle excitation timing, the optimization allowed substantial negative muscle work to occur,

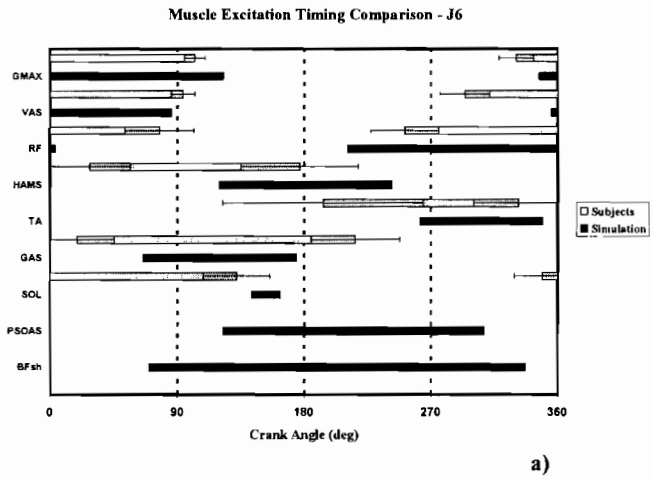

a)

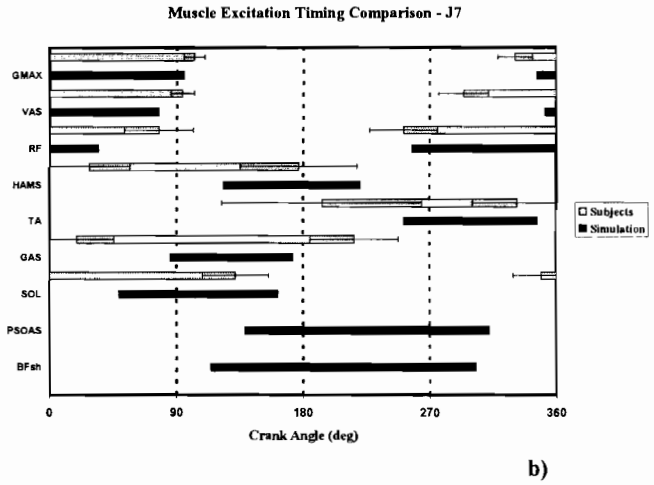
Muscle Excitation Timing Comparison - J7
GMAX
VAS
RF
HAMS
TA
GAS
SOL
PSOAS
BFsh
Subjects
Simulation
Crank Angle (deg)

b)

Fig. 4 Muscle excitation timing comparison between the subject's mean data (Neptune et al., 1997) and (*a*) criterion J6 and (*b*) criterion J7. Error bars indicate ±1 standard deviation.

especially for the BFsh and PSOAS muscles when they were excited during the mid-downstroke while lengthening. Including the EMG timing in the performance criterion reduced the amount of negative muscle work and improved the match with the experimental data. These results suggest that minimizing negative muscle work may be important in endurance cycling.

To test this hypothesis, a post-hoc criterion was formulated that only minimized the amount of negative muscle power used within the optimization framework. Although not presented in this study, the results showed that while this criterion reproduced the major features of the subject's pedaling mechanics, the rms errors for the kinetic and kinematic quantities were nearly twice the errors of criterion J7. These results indicate that minimizing negative work is not the only objective of the central nervous system during pedaling and indicate the need

Table 2 Kinetic, kinematic, and EMG timing rms errors for each performance criterion evaluated

Quantity	J1	J2	J3	J4	J5	J6	J7
Pedal Angle	22.5	18.1	17.6	2.6	9.4	5.2	8.2
Pedal Force (Fx)	6.1	17.8	29.0	16.0	21.9	12.5	12.3
Pedal Force (Fy)	5.7	6.3	15.2	6.8	10.2	5.4	4.6
Crank Torque	7.8	3.2	11.9	4.3	5.7	4.1	5.3
Hip Moment	19.8	9.6	3.5	9.4	4.9	8.7	8.6
Knee Moment	11.4	11.0	4.6	9.7	5.5	9.9	8.5
Ankle Moment	15.5	11.2	6.7	8.5	7.3	7.7	8.6
EMG Timing Error	10.7	13.2	12.5	13.7	11.8	13.4	10.1
Total Error	99.5	90.4	101.0	71.0	76.7	66.9	66.3